

Submitted to  
*Nuclear Instruments and Methods in Physics Research B*

## MeV-ion beam analysis of the interface between filtered cathodic arc-deposited a-carbon and single crystalline silicon

T. Kamwanna <sup>a</sup>, N. Pasaja <sup>b</sup>, L.D. Yu <sup>a</sup>, T. Vilaithong <sup>a</sup>, A. Anders <sup>c</sup>, S. Singkarat <sup>a</sup>

<sup>a</sup> Fast Neutron Research Facility, Department of Physics, Faculty of Science, Chiang Mai University, Chiang Mai 50200, Thailand

<sup>b</sup> Department of Physics, Faculty of Science, Mahasarakham University, Mahasarakham 44150, Thailand

<sup>c</sup> Lawrence Berkeley National Laboratory, University of California, Berkeley, CA 94720, USA

1 August 2008

A. Anders was supported by the U.S. Department of Energy under Contract No. DE-AC02-05CH11231. The authors would like to express their gratitude to the National Research 3 Council of Thailand (NRCT) and the International Atomic Energy Agency 4 (IAEA, Vienna) for providing financial support. T. Kamwanna is deeply grateful to the scholarship from the Development and Promotion of Science and Technology Talents Project (DPST). N. Pasaja wishes to thank the RGJ Ph.D. scholarship of the Thailand Research Fund. We thank Mr. C. Thongleurm of the Institute for Science and Technology Research and Development, Chiang Mai University, for technical assistance.

This document was prepared as an account of work sponsored in part by the United States Government. While this document is believed to contain correct information, neither the United States Government nor any agency thereof, nor The Regents of the University of California, nor any of their employees, makes any warranty, express or implied, or assumes any legal responsibility for the accuracy, completeness, or usefulness of any information, apparatus, product, or process disclosed, or represents that its use would not infringe privately owned rights. Reference herein to any specific commercial product, process, or service by its trade name, trademark, manufacturer, or otherwise, does not necessarily constitute or imply its endorsement, recommendation, or favoring by the United States Government or any agency thereof, or The Regents of the University of California. The views and opinions of authors expressed herein do not necessarily state or reflect those of the United States Government or any agency thereof or The Regents of the University of California.

1  
2  
3  
4  
5  
6  
7  
8  
9  
10  
11  
12  
13  
14  
15  
16  
17  
18  
19  
20  
21  
22  
23  
24  
25  
26  
27  
28  
29  
30  
31  
32  
33  
34  
35  
36  
37  
38

# MeV-ion beam analysis of the interface between filtered cathodic arc-deposited *a*-carbon and single crystalline silicon

T. Kamwanna<sup>a,\*</sup> N. Pasaja<sup>b</sup> L.D. Yu<sup>a</sup> T. Vilaithong<sup>a</sup>  
A. Anders<sup>c</sup> S. Singkarat<sup>a</sup>

<sup>a</sup>*Fast Neutron Research Facility, Department of Physics, Faculty of Science,  
Chiang Mai University, Chiang Mai 50200, Thailand*

<sup>b</sup>*Department of Physics, Faculty of Science, Mahasarakham University,  
Mahasarakham 44150, Thailand*

<sup>c</sup>*Lawrence Berkeley National Laboratory, University of California, Berkeley, CA  
94720, USA*

---

## Abstract

Amorphous carbon (*a*-C) films were deposited on Si(100) wafers by a filtered cathodic vacuum arc (FCVA) plasma source. A negative electrical bias was applied to the silicon substrate in order to control the incident energy of carbon ions. Effects of the electrical bias on the *a*-C/Si interface characteristics were investigated by using standard Rutherford backscattering spectrometry (RBS) in the channeling mode with 2.1-MeV He<sup>2+</sup> ions. The shape of the Si surface peaks of the RBS/channeling spectra reflects the degree of interface disorder due to atomic displacement from the bulk position of the Si crystal. Details of the analysis method developed are described. It was found that the width of the *a*-C/Si interface increases linearly with the substrate bias voltage but not the thickness of the *a*-C film.

1  
2  
3  
4  
5  
6  
7  
8  
9  
10  
11  
12  
13  
14  
15  
16  
17  
18  
19  
20  
21  
22  
23  
24  
25  
26  
27  
28  
29  
30  
31  
32  
33  
34  
35  
36  
37  
38  
39  
40  
41  
42  
43  
44  
45  
46  
47  
48  
49  
50  
51  
52  
53  
54  
55  
56  
57  
58  
59  
60  
61  
62  
63  
64  
65

*Key words:* Rutherford backscattering spectrometry (RBS), Channeling,  
Amorphous carbon, Interface, Filtered cathodic vacuum arc (FCVA)  
*PACS:* 82.80.Yc, 61.85.+p, 81.05.Uw, 81.15.-z

---

\* Corresponding author address: Tel.: +66 53 943379; Fax: +66 53 222776.  
*Email address:* teerasak@fnrf.science.cmu.ac.th (T. Kamwanna).

1  
2  
3  
4 **1 Introduction**  
5  
6  
7  
8

9 Amorphous carbon (*a*-C) has been of great interest for its outstanding me-  
10 chanical and electrical properties, such as wide band gap, high hardness, wear  
11 resistance and optical transparency [1,2]. These unique properties have been  
12 fascinated for numerous applications. In general, the *a*-C films exhibit a vari-  
13 ety of structural features and properties that depend on the fraction of  $sp^3$  and  
14  $sp^2$  bonding in the films. It is well known that *a*-C films deposited by cathodic  
15 arc plasma have large compressive stress correlated with a higher fraction of  
16 the  $sp^3$  bonding, which leads to poorer adhesion, especially when a thicker  
17 film is required. The fraction of the  $sp^3$  bonding depends on the incident en-  
18 ergy of carbon ions that strike on growing carbon films [3]. Higher energy of  
19 carbon ions ( $> 200$  eV) can reduce the compressive stress, thus adhesion is  
20 improved, which is correlated to the transformation of  $sp^3$  to  $sp^2$  bonding [3].  
21 In order to control the incident ion energy, a negatively dc or pulse bias volt-  
22 age was applied to the substrate [4]. The understanding of its effect on the  
23 film properties is of technological importance [5,6].  
24  
25  
26  
27  
28  
29  
30  
31  
32  
33  
34  
35  
36  
37  
38  
39  
40  
41  
42

43 A broad range of surface sensitive techniques [5–10] have been used to char-  
44 acterize the interface morphology of an *a*-C film on a crystalline substrate.  
45 However, the information obtained from these techniques are qualitative. Fol-  
46 lowing to the fact that ion scattering is extremely sensitive to the top most  
47 atomic layer, MeV He ion beam backscattering was used in this work as a  
48 means of studying the interface morphology of a thin *a*-C film on a single  
49 crystal silicon (100) substrate in a non-destructive manner. The channeling  
50 phenomenon of He ions along the  $\langle 100 \rangle$  axial direction of the Si substrate is  
51 utilized in order to highlight the surface peak, which is sensitive to the degree  
52  
53  
54  
55  
56  
57  
58  
59  
60  
61  
62  
63  
64  
65

1  
2  
3  
4 of disorder of Si atoms around the subsurface region. Thus, this surface peak  
5  
6 reflects the situation at the *a*-C layer/substrate interface, which is in turn  
7  
8 related to the electrical bias to the Si substrate. Moreover, channeling phe-  
9  
10 nomenon is used to suppress the background intensity of Si backscattering so  
11  
12 that backscattering yield from C target is sufficiently well resolved to analyze  
13  
14 the peak area. Therefore, the ion channeling measurement has advantage over  
15  
16  
17 those techniques especially in its quantitative reliability.  
18  
19  
20  
21  
22

## 23 **2 Experimental**

### 24 *2.1 Sample preparation*

25  
26  
27  
28  
29  
30  
31  
32 Amorphous carbon films were fabricated by filtered cathodic vacuum arc  
33  
34 (FCVA) plasma at room temperature where the carbon plasma was obtained  
35  
36 from a 99.995% pure graphite cathode. The FCVA system has been described  
37  
38 in detail elsewhere [11]. In brief, the FCVA source was operated in pulse mode  
39  
40 based on 10-sections of pulse forming network (PFN) with pulse duration of  
41  
42 about 120 s and pulse arc current exceeding 200 A depending on charging  
43  
44 voltage to PFN [12]. This experimental pulse arc current was kept at about  
45  
46 572 A with a repetition rate of 2 pps for all samples made. *P*-type Si (100)  
47  
48 wafers were used as substrates. Prior to depositing *a*-C films, the substrates  
49  
50 were cleaned by following the standard RCA procedure [13]. A dc bias voltage  
51  
52 ( $V_b$ ) ranging from -0.2 to -2.0 kV were applied to the substrate holder during  
53  
54 deposition in order to increase the incident ion energy. A solenoid filter was  
55  
56 used to remove macroparticles. The energy of carbon ions (in eV) was directly  
57  
58 related to the bias voltage (in V) because only singly charged carbon ions were  
59  
60  
61  
62  
63  
64  
65

1  
2  
3  
4 in the plasma. The substrate holder was placed at about 15 cm from an exit  
5  
6 of the filter. The vacuum chamber was evacuated to a base pressure of about  
7  
8  $6 \times 10^{-6}$  mbar by a cryogenic pump.  
9

## 10 11 12 13 14 15 16 4 *2.2 Backscattering measurements* 17 18 19 20

21 The interface morphology of thin *a*-C films was investigated by means of  
22  
23 Rutherford backscattering spectrometry in the channeling mode (abbreviated  
24  
25 as RBS/C hereafter) [14,15]. The analysis was performed utilizing 2.1-MeV  
26  
27  $\text{He}^{2+}$  beam produced by the 1.7-MV Tandetron accelerator at Chiang Mai  
28  
29 University. The typical ion beam current on the sample was 15 nA. A max-  
30  
31 imum beam divergence was less than  $0.05^\circ$  with a diameter of 1 mm. Two  
32  
33 small permanent magnets were placed in parallel in front of the sample holder  
34  
35 for acting as a secondary electron suppressor, enabling accurate monitoring of  
36  
37 ion beam charge on the sample. Backscattered  $\text{He}^{2+}$ -ions were detected by a  
38  
39 standard silicon surface barrier (SSB) detector with an energy resolution of 12  
40  
41 keV positioned at  $115^\circ$  with respect to the beam direction. For the channeling  
42  
43 measurements, the samples were mounted on a goniometer with two tilting  
44  
45 axes which were automatically adjusted in both angles by a computer-based  
46  
47 control until a minimum in the axial channeling yield was observed. In order  
48  
49 to avoid crystal or film damage due to the analyzing beam, a fresh spot was  
50  
51 chosen after each searching procedure. The measuring period of all the RBS/C  
52  
53 spectra was controlled by keeping the same value of total  $\text{He}^{2+}$  charge accumu-  
54  
55 lation on each target in order to reduce the influence of the  $\text{He}^{2+}$  bombarding  
56  
57 fluence on the dechanneling.  
58  
59  
60  
61  
62  
63  
64  
65

1  
2  
3  
4 **3 Results and discussions**  
5  
6  
7

8  
9 2 Typical 2.1 MeV random and aligned RBS spectra from the as-grown *a*-C thin  
10 3 film on the Si (100) substrate are shown in Fig. 1. The channeling phenomenon  
11 4 allows us to see the nonshadowed Si atoms of the surface layer more clearly  
12 5 since ions scattered by these atoms appear as a surface peak while those  
13 6 crystalline atoms underneath are almost hidden. This effect also enhances the  
14 7 C-peak that comes from the deposited layer of *a*-C on top of the Si surface. As  
15 8 shown in Fig. 1, the clarity of the C-peak is far better in the aligned spectrum  
16 9 than in the random spectrum. Quantitative evaluation is possible only from  
17 10 the aligned spectrum.  
18  
19  
20  
21  
22  
23  
24  
25  
26  
27  
28  
29  
30  
31

32 11 *3.1 Interface disorder, qualitative analysis*  
33  
34  
35  
36

37 12 In Fig. 2, the ion channeling spectra obtained from *a*-C thin films deposited  
38 13 on Si(100) wafers are compared for different bias voltages. In this case, the  
39 14 surface peaks around channel number 516 reflect the distribution of those non-  
40 15 shadowed Si atoms. As seen here, the Si surface peaks are increased both in  
41 16 width and height with the substrate bias voltage. The increment of this surface  
42 17 peak is related to the increasing number of displaced Si atoms at around the  
43 18 top layer of Si substrate since major lattice damage builds up in the substrate  
44 19 with increasing irradiation energy. For the first period of deposition, energetic  
45 20 C<sup>+</sup>-ions of a few keV can effectively induce displacement of the Si atoms from  
46 21 their original lattice sites due to a low displacement energy of about 38 eV  
47 22 [16]. It is noticed that the front edges of the Si surface peaks slightly shift to  
48 23 lower energy. This fact will be discussed later and utilized for calculation of  
49  
50  
51  
52  
53  
54  
55  
56  
57  
58  
59  
60  
61  
62  
63  
64  
65

1  
2  
3  
4 the film thickness.  
5  
6  
7  
8  
9

10 *3.2 Oxide analysis*  
11  
12  
13  
14

15 Prior to quantitative analysis of the interface disorder, the surface oxidation  
16 situation must be first clarified as surface oxide would affect the Si surface  
17 peak of the aligned spectrum. From Fig. 2, no apparent oxygen peak was  
18 observed at around channel 355. This could be an indication of a native oxide  
19 ( $\text{SiO}_2$ ) free surface of the substrate. The oxide might have successfully been  
20 removed following the HF dip. We confirmed this assumption by using the  
21 non-Rutherford scattering cross-section effect in the  $^{16}\text{O}(\alpha,\alpha)^{16}\text{O}$  reaction to  
22 enhance O-backscattering yield. The deviations of the scattering cross-section  
23 from the Rutherford formula are observed for He ion energies above 2.25 MeV  
24 scattered from oxygen atoms [17]. There are resonances at 2.5 MeV and 3.05  
25 MeV. Prior to ion scattering measurements, an energy scan was conducted in  
26 order to calibrate the  $\text{He}^{2+}$ -ion energy to the centroid of the  $^{16}\text{O}(\alpha,\alpha)^{16}\text{O}$  3.05  
27 MeV nuclear resonance via the oxygen signal from an alumina ( $\text{Al}_2\text{O}_3$ ) sample.  
28 This effect is demonstrated in Fig. 3 for the oxygen peak measured at 3.05  
29 MeV using not cleaned and cleaned Si wafers with the treatment mentioned  
30 earlier. The oxygen peak is clearly visible, at resonance energy, only from not  
31 cleaned Si. The two spectra of not cleaned sample shown in Fig. 3 correspond  
32 to the same sample measured at the resonant energy 3.05 MeV and at about 15  
33 keV off resonance. The sensitivity of RBS to oxygen in the not cleaned sample  
34 can be further enhanced by a factor of about 15 due to a higher cross-section  
35 than given by the Rutherford formula at  $165^\circ$  backscattering angle [17]. Thus,  
36 it is certain that those Si surface peaks are corresponding only to Si atoms at  
37  
38  
39  
40  
41  
42  
43  
44  
45  
46  
47  
48  
49  
50  
51  
52  
53  
54  
55  
56  
57  
58  
59  
60  
61  
62  
63  
64  
65



1  
2  
3  
4 around the outermost layers of the clean Si crystal or the disordered *a*-C/Si  
5  
6 interface.  
7  
8  
9

10  
11 3.3 *Interface disorder as a function of deposition bias voltage, quantitative*  
12  
13 *analysis*  
14

15  
16  
17 To understand the measurement collected in the context of disorder distribu-  
18  
19 tion, we provide a brief description of some basic channeling concept. In the  
20  
21 framework of the two-beam approximation model [18,19], the normalized yield  
22  
23 at depth  $x$ ,  $\chi(x)$ , is given by [14]  
24  
25

26  
27 
$$\chi(x) = \chi_R(x) + [1 - \chi_R(x)] [N_D(x)/N], \quad (1)$$
  
28  
29  
30

31 where  $\chi_R(x)$  is the dechanneled part of the beam,  $N_D(x)$  represents the total  
32  
33 displaced atom density at depth  $x$  and  $N$  is the atomic density of the crystal.  
34  
35 In this work, the amount of displaced atoms is not too high due to the low  
36  
37 irradiation energy. Therefore, it is possible to make a simple estimation to  
38  
39 obtain the fraction  $\chi_R(x)$  by using the single scattering approximation [14],  
40  
41 as approximated by  
42  
43  
44

45 
$$\chi_R(x) = \chi_V(x) + [1 - \chi_V(x)] P(x, \psi_{1/2}), \quad (2)$$
  
46  
47  
48  
49

50 where  $\chi_V(x)$  is the normalized aligned yield from a virgin crystal and  $P(x, \psi_{1/2})$   
51  
52 is the probability that the channeled ions are dechanneled by the disorder in  
53  
54 the region between the surface down to the depth  $x$  through angles greater  
55  
56 than the critical angle  $\psi_{1/2}$ . By using Eqs. 1 and 2, we can calculate the depth  
57  
58 profile of the displaced atoms  $N_D(x)$ . Conversion from the channel number  
59  
60 to the corresponding depth is carried out following the standard procedure  
61  
62  
63  
64  
65

1 [14,17] based on the geometry of the measurements and the stopping power  
2 given by Ziegler [20].

3 With the method mentioned, the quantitative disorder can be extracted from  
4 those RBS/C spectra. Fig. 4 shows displaced Si atom depth profiles as a func-  
5 tion of the substrate bias voltage. Gaussian-like disorder profiles are observed.  
6 The profile increases both in height and depth into the Si substrate with in-  
7 creasing substrate bias voltage. Also, the total number of displaced Si atoms  
8 in the unit area of the disorder profiles in Fig. 4a increases with increasing sub-  
9 strate bias voltage, as shown in Fig. 4b. This fact indicates that the substrate  
10 bias voltage is directly associated with the carbon ion energy, as expected,  
11 which causes the ions to penetrate deeper and the substrate atoms to have  
12 more displacements. The inset of Fig. 4a shows the depth profiles of C-ions  
13 and displacement of Si atoms calculated by the Monte Carlo SRIM simulation  
14 program [21] for 2-keV C-ions implanted in Si. The distribution of C atoms has  
15 nearly a Gaussian shape with a projected range of 9.5 nm while the displace-  
16 ment peak is located closer to the surface at about 4.5 nm with a long damage  
17 tail stretching into the whole C distribution region. According to SRIM simu-  
18 lations, the displacement of atoms in the host crystal depends on two factors:  
19 the collision between the incident ions and atoms in the host material and  
20 the recoil processes of incident ions. The experimental result shows that the  
21 position of the displaced atom profile is similar to that of the C distribution;  
22 and it can be interpreted that the lattice disorder of Si atoms is mostly due  
23 to the implantation of C-ions.

1  
2  
3  
4 3.4 Carbon film characteristics  
5  
6  
7  
8

9 2 By virtue of the RBS/C spectra in Fig. 2, the Si surface peaks are slightly  
10 3 shifted from the surface peak of the clean Si(100) surface towards lower backscat-  
11 4 tered ion energy due to the energy loss of He<sup>2+</sup>-ions in traversing the *a*-C front  
12 5 layer. Therefore, the energy difference  $\Delta E$  between He<sup>2+</sup>-ions scattered from  
13 6 the surface of clean Si and those scattered from the C/Si interface is related  
14 7 to the thickness of the film. By referring to the known stopping cross section  
15 8 factor and the experimental parameter of the scattering geometry, we can  
16 9 convert the energy difference  $\Delta E$  to the *a*-C film thickness with the known  
17 10 mass density of the FCVA-deposited *a*-C films [22]. In addition, the C-peaks  
18 11 in RBS/C spectra refer to the carbon atoms from the deposited layer of *a*-  
19 12 C on the Si surface as well as the mixed layer of Si and C caused by the  
20 13 energetic C-ion irradiation. Thus, the total numbers of counts within these  
21 14 C-peaks were considered. The integrated area of the C-peak was evaluated by  
22 15 a straight-line extrapolation of the contribution from the Si substrate. The  
23 16 conversion of measured area to the C film thickness is made by comparison  
24 17 with the height of a random spectrum for Si [14]. From these results, we can  
25 18 estimate the thickness of the intermixed layer, which is the same as the width  
26 19 of the *a*-C/Si interface, from the difference between the total carbon thickness  
27 20 and the *a*-C film thickness.  
28  
29  
30  
31  
32  
33  
34  
35  
36  
37  
38  
39  
40  
41  
42  
43  
44  
45  
46  
47  
48  
49  
50

51 Fig. 5 shows the width of the *a*-C/Si interface as a function of C<sup>+</sup>-ion energy  
52 21 for the total C thickness of about 22 nm. The thickness of the *a*-C/Si interface  
53 22 increases from 0.8 nm at zero bias to 8.9 nm when ion energy is equivalent  
54 23 to 2 keV. This behavior indicates that the width of the *a*-C/Si interface is  
55 24 mainly affected by the carbon ion energy.  
56 25  
57  
58  
59  
60  
61  
62  
63  
64  
65

1  
2  
3  
4 To make this point more clear, we compare our results with  $C^+$ -ion ranges  
5  
6 in virgin Si for the energy range of 0.2-2 keV as calculated by the SRIM  
7  
8 simulation program. As shown in Fig. 5, the widths of the  $a$ -C/Si interface  
9  
10 follow the same trend as the ion range although they are all narrower. This  
11  
12 is because in a real situation, the incident  $C^+$ -ions lose their initial kinetic  
13  
14 energy to a greater extent when the carbon layer grows thicker. Thus the  $C^+$ -  
15  
16 ions enter the Si substrate region with less energy when the carbon irradiation  
17  
18 (deposition) time increasing. For example, the  $C^+$ -ions, of initial energy 1 keV,  
19  
20 can penetrate into the Si substrate to a depth of around 5.7 nm at the most, at  
21  
22 the first instant of irradiation. After that the penetration depth continuously  
23  
24 decreases to zero within about 3 minutes since the carbon layer has grown  
25  
26 thicker than 3.8 nm, which is the range of  $C^+$ -ions in carbon film according  
27  
28 to SRIM. This behavior indicates that the interface width should be smaller  
29  
30 than the ion range, and explains the evidence from Fig. 5 that no significant  
31  
32 changes are seen in the interface width of the two different deposition times  
33  
34 for the same ion energies.  
35  
36  
37  
38  
39  
40  
41  
42

### 17 3.5 Overview of the Si-C interface including total C

18 To obtain a more quantitative picture of the  $a$ -C/Si structure, we suggest a  
19  
20 model that summarize the experimental observations and our interpretation  
21  
22 of the results as shown in Fig. 6 for the  $V_b = -2$  kV case. The depth profile of C  
23  
24 atoms was extracted from the C-peak by following the standard procedure [14].  
25  
26 A Gaussian distribution is observed and the total C thickness is obtained from  
27  
28 full width at half maximum (FWHM) of the profile. As previously mentioned,  
29  
30 the distribution of carbon can be divided into two regions. The first one is the  
31  
32  
33  
34  
35  
36  
37  
38  
39  
40  
41  
42

1  
2  
3  
4 1 region where the carbon ions penetrate a certain distance in the Si substrate  
5  
6 2 and knock some of Si atoms out of their bulk lattice position resulting in the  
7  
8 3 interface disorder. The formation of *a*-C/Si interface at the near surface of Si is  
9  
10 4 affected by the energy of carbon ions at the initial stage of growth. The second  
11  
12 5 region is the deposited carbon film on the top of the *a*-C/Si interface. This  
13  
14 6 region represents the *a*-C film. As seen here, the tail of the disorder profile  
15  
16 7 is slightly stretched into the *a*-C film region. This suggests that the Si atoms  
17  
18 8 were "sputtered" by those carbon ions but retained by the thin film on top.  
19  
20  
21  
22  
23  
24  
25  
26  
27  
28  
29  
30  
31  
32

## 33 9 4 Conclusions

34  
35  
36  
37  
38

39 10 The characteristics of the interface between the low-energy FCVA-deposited  
40  
41 11 *a*-C film and the single crystalline Si substrate have been studied in detail  
42  
43 12 with MeV-ion beam analysis, particularly the RBS/C technique. Relevant  
44  
45 13 measurement methods based on the RBS/C spectra have been developed.  
46  
47 14 Quantitative information on the interface and the film has been obtained from  
48  
49 15 the measurements, including the disorder depth profile in the Si substrate,  
50  
51 16 total carbon profile, carbon film thickness and carbon ions penetrated in the  
52  
53 17 interface, which are all in the nano-scale. The overview of the interface that  
54  
55 18 contains the implanted carbon and displaced silicon atoms together with the  
56  
57 19 deposited carbon film shows that the interface expands with increasing of the  
58  
59 20 C-ion energy or the substrate bias voltage.  
60  
61  
62  
63  
64  
65

1  
2  
3  
4 **Acknowledgements**  
5  
6  
7

8  
9 2 The authors would like to express their gratitude to the National Research  
10  
11 3 Council of Thailand (NRCT) and the International Atomic Energy Agency  
12  
13 4 (IAEA, Vienna) for providing financial support. T. Kamwanna is deeply grate-  
14  
15 5 ful to the scholarship from the Development and Promotion of Science and  
16  
17 6 Technology Talents Project (DPST). N. Pasaja wishes to thank the RGJ Ph.D.  
18  
19 7 scholarship of the Thailand Research Fund. We thank Mr. C. Thongleurm of  
20  
21 8 Institute for Science and Technology Research and Development, Chiang Mai  
22  
23 9 University for technical assistance. This work was supported by the U.S. Department of  
24  
25 of Energy under Contract No. DE-AC03-05CH11231.  
26  
27  
28

29  
30 **References**  
31  
32  
33

- 34 [1] J. Robertson, Mater. Sci. Eng: R: Rep 37 (2002) 129.  
35  
36  
37 [2] A.A. Voevodin, J.S. Zabinski, Thin Solid Films 370 (2000) 223.  
38  
39  
40 [3] P.J. Fallon, V.S. Veerasamy, C.A. Davis, J. Robertson, G.A.J. Amaratunga,  
41  
42 W.I. Milne, J. Koskinen, Phys. Rev. B 48 (1993) 4777.  
43  
44  
45 [4] J.Y. Sze, B.K. Tay, D. Sheeja, S.P. Lau, Y.Q. Fu, Daniel H.C. Chua, W.I. Milne,  
46  
47 Thin Solid Films 447-448 (2004) 148.  
48  
49  
50 [5] N.A. Hastas, C.A. Dimitriadis, P. Patsalas, Y. Panayiotatos, D.H. Tassis, S.  
51  
52 Logothetides, J. Appl. Phys. 89 (2001) 2832.  
53  
54  
55 [6] P. Patsalas, S. Logothetidis, P.C. Kelires, Diamond Relat. Mater. 14 (2005)  
56  
57 1241.  
58  
59  
60 [7] I. Montero, L. Galán, F. Rueda, J. Perrière, Surf. Sci. 298 (1993) 79.  
61  
62  
63  
64  
65

- 1  
2  
3  
4 [8] O. Böhme, A. Cebollada, S. Yang, D.G. Teer, J.M. Albella, E. Román, J. Appl.  
5  
6 Phys. 88 (2000) 1861.  
7  
8  
9 [9] S. Logothetidis, E. Evangelon, N. Konofaos, J. Appl. Phys. 82 (1997) 5017.  
10  
11 [10] C.A. Davis, K.M. Knowles, G.A.J. Amaratunga, Surf. Coat. Technol. 76-77  
12  
13 (1995) 316.  
14  
15  
16 [11] A. Anders, R.A. MacGill, T.A. McVeigh, Rev. Sci. Instrum. 70 (1999) 4532.  
17  
18  
19 [12] N. Pasaja, S. Sansongsiri, S. Intarasiri, T. Vilaithong, A. Anders, Nucl. Instr.  
20  
21 and Meth. B259 (2007) 867.  
22  
23  
24 [13] W. Kern, D.A. Puotinen, RCA Rev. 31 (1970) 187.  
25  
26 [14] W.K. Chu, J.W. Mayer, Marc-A. Nicolet, Backscattering Spectrometry,  
27  
28 Academic Press, New York, 1978.  
29  
30  
31 [15] L.C. Feldman, J.W. Mayer, S.T. Picraux, Materials Analysis by Ion Channeling,  
32  
33 Academic Press, New York, 1982.  
34  
35  
36 [16] G. Lucas, L. Pizzagalli, Phys. Rev. B 72 (2005) 161202.  
37  
38 [17] J.R. Tesmer, M.A. Nastasi (eds.), Handbook of Modern Ion Beam Material  
39  
40 Analysis, Materials Research Society, Pittsburgh, PA, 1995.  
41  
42  
43 [18] E. Bøgh, Phys. Rev. Lett. 19 (1967) 61.  
44  
45  
46 [19] E. Albertazzi, M. Bianconi, G. Lulli, R. Nipoti, M. Cantiano, Nucl. Instr. and  
47  
48 Meth. B 118 (1996) 128.  
49  
50  
51 [20] J.F. Ziegler, The Stopping and Ranges of Ions in Matter, Volume 4, Pergamon  
52  
53 Press, New York, 1977.  
54  
55 [21] SRIM Program, <http://www.srim.org>.  
56  
57  
58 [22] A. Anders, N. Pasaja, S.H.N. Lim, T.C. Petersen, V.J. Keast, Surf. Coat.  
59  
60 Technol. 201 (2007) 4628.  
61  
62  
63  
64  
65

1  
2  
3  
4  
5  
6  
7  
8  
9  
10  
11  
12  
13  
14  
15  
16  
17  
18  
19  
20  
21  
22  
23  
24  
25  
26  
27  
28  
29  
30  
31  
32  
33  
34  
35  
36  
37  
38  
39  
40  
41  
42  
43  
44  
45  
46  
47  
48  
49  
50  
51  
52  
53  
54  
55  
56  
57  
58  
59  
60  
61  
62  
63  
64  
65

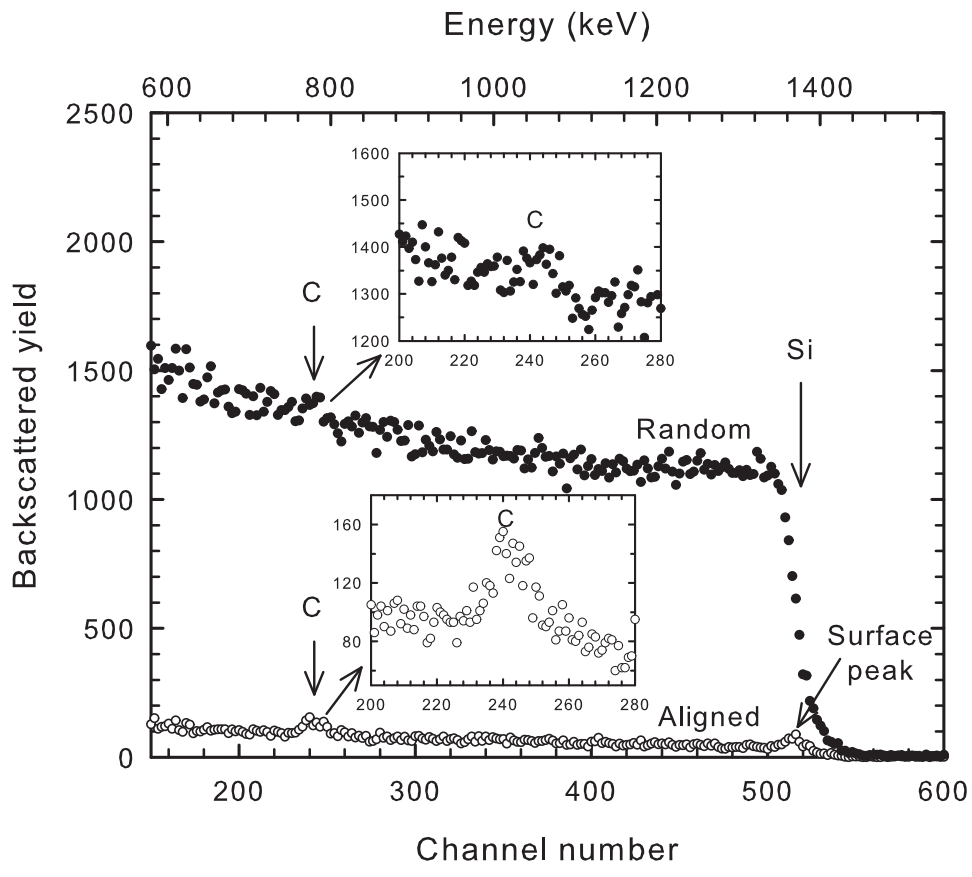


Fig. 1. Comparison of random and channeled  $\langle 100 \rangle$  RBS spectra of the Si(100) wafer with a 3 nm thick  $a$ -C film on top. Vertical arrows indicate the expected position of  $\text{He}^{2+}$ -ions backscattered from C and Si atoms on the surface. The insets show details in the C-peak region of both spectra.



1  
2  
3  
4  
5  
6  
7  
8  
9  
10  
11  
12  
13  
14  
15  
16  
17  
18  
19  
20  
21  
22  
23  
24  
25  
26  
27  
28  
29  
30  
31  
32  
33  
34  
35  
36  
37  
38  
39  
40  
41  
42  
43  
44  
45  
46  
47  
48  
49  
50  
51  
52  
53  
54  
55  
56  
57  
58  
59  
60  
61  
62  
63  
64  
65

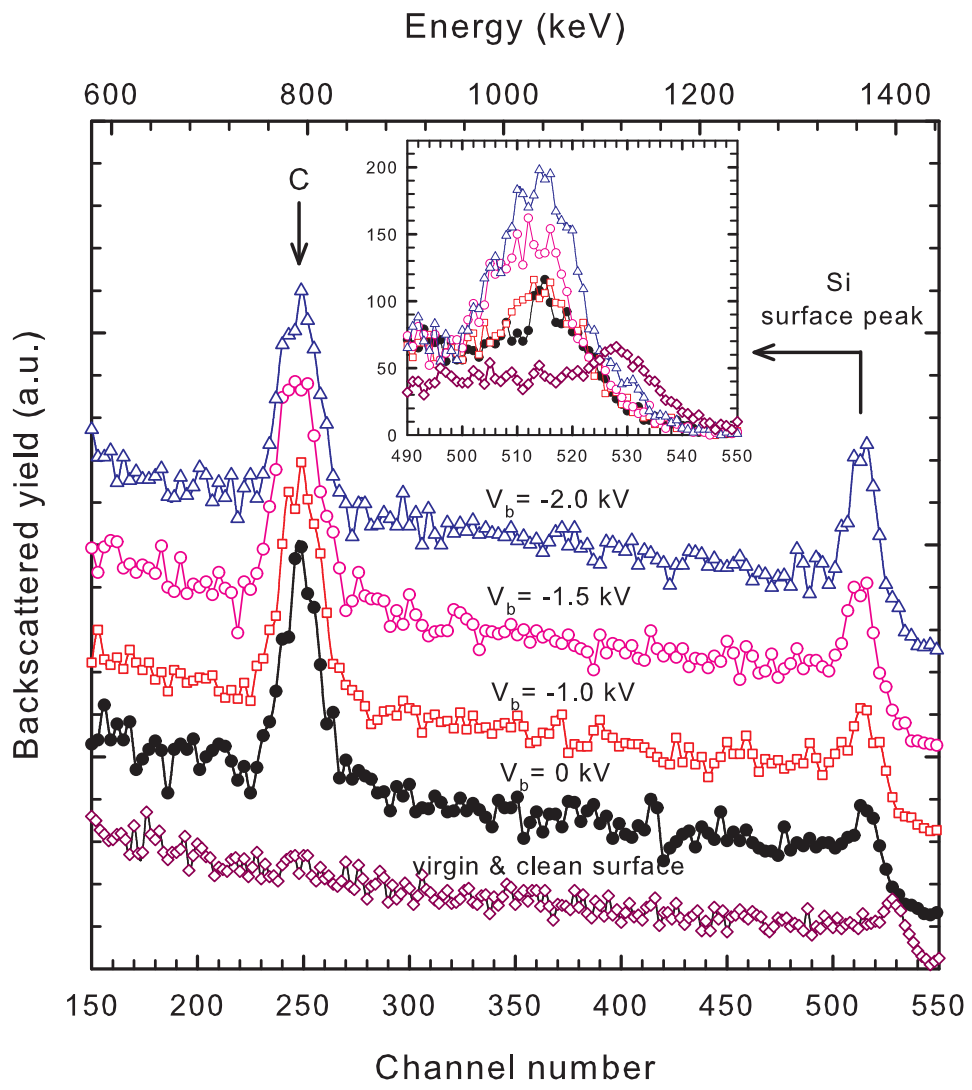


Fig. 2. Measured RBS/C spectra of a 2.1-MeV  $\text{He}^{2+}$  beam aligned along the  $\langle 100 \rangle$  axial direction of Si wafers deposited with  $a$ -C layers at 4 different bias voltages but with the same deposition time. The inset enlarges the Si surface peaks. As a reference, the backscattering yield spectrum along the  $\langle 100 \rangle$  axis of a virgin Si wafer is also included.

1  
2  
3  
4  
5  
6  
7  
8  
9  
10  
11  
12  
13  
14  
15  
16  
17  
18  
19  
20  
21  
22  
23  
24  
25  
26  
27  
28  
29  
30  
31  
32  
33  
34  
35  
36  
37  
38  
39  
40  
41  
42  
43  
44  
45  
46  
47  
48  
49  
50  
51  
52  
53  
54  
55  
56  
57  
58  
59  
60  
61  
62  
63  
64  
65

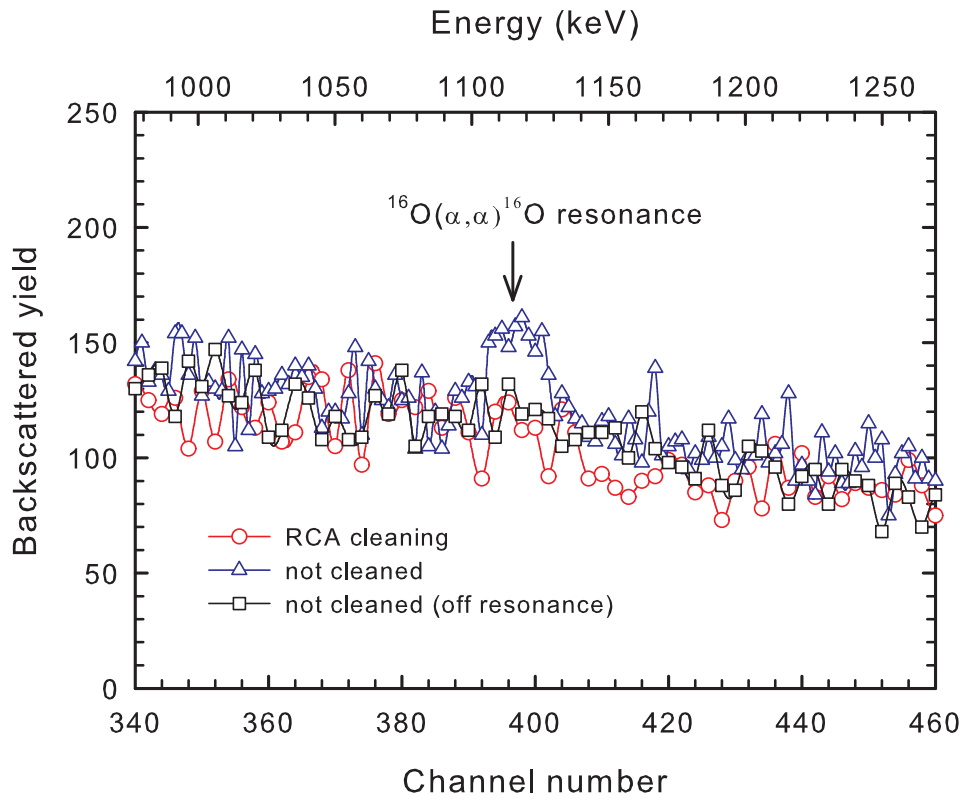


Fig. 3. RBS/C spectra comparing the cleaned and not cleaned silicon wafers at the resonance energy of 3.05 MeV and the same not cleaned sample collected at the about 15 keV off resonance.

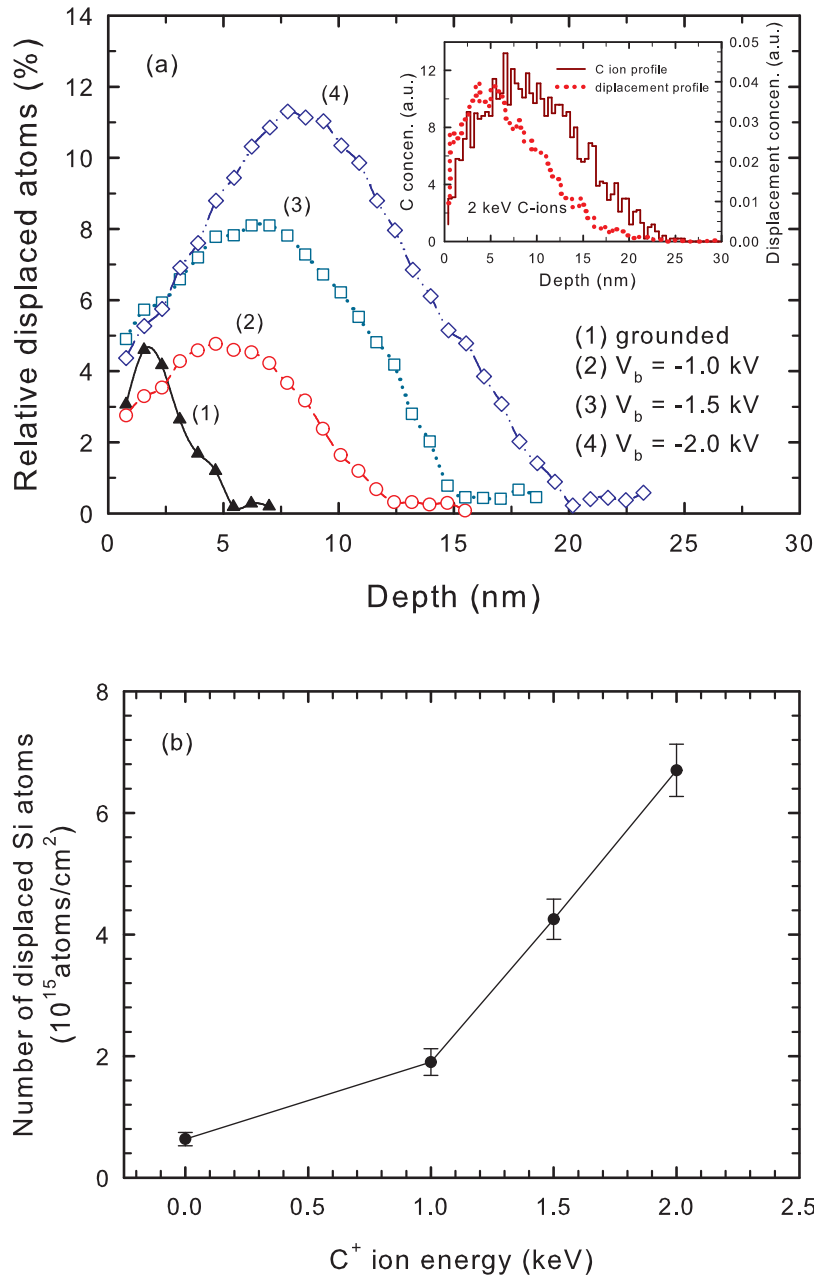


Fig. 4. Analysis of displaced Si atoms as a function of the substrate bias voltage. (a) The measured relative concentration of displaced atoms ( $N_D/N$ ) in the surface peak of Si wafers deposited with *a*-C layers as a function of substrate bias voltage. The inset shows the C-ion (histogram) and displacement (dotted line) profile for 2 keV C<sup>+</sup>-ions calculated by SRIM. (b) The total number of displaced Si atoms in the interface as a function of substrate bias voltage. The solid line is given for reference.

1  
2  
3  
4  
5  
6  
7  
8  
9  
10  
11  
12  
13  
14  
15  
16  
17  
18  
19  
20  
21  
22  
23  
24  
25  
26  
27  
28  
29  
30  
31  
32  
33  
34  
35  
36  
37  
38  
39  
40  
41  
42  
43  
44  
45  
46  
47  
48  
49  
50  
51  
52  
53  
54  
55  
56  
57  
58  
59  
60  
61  
62  
63  
64  
65

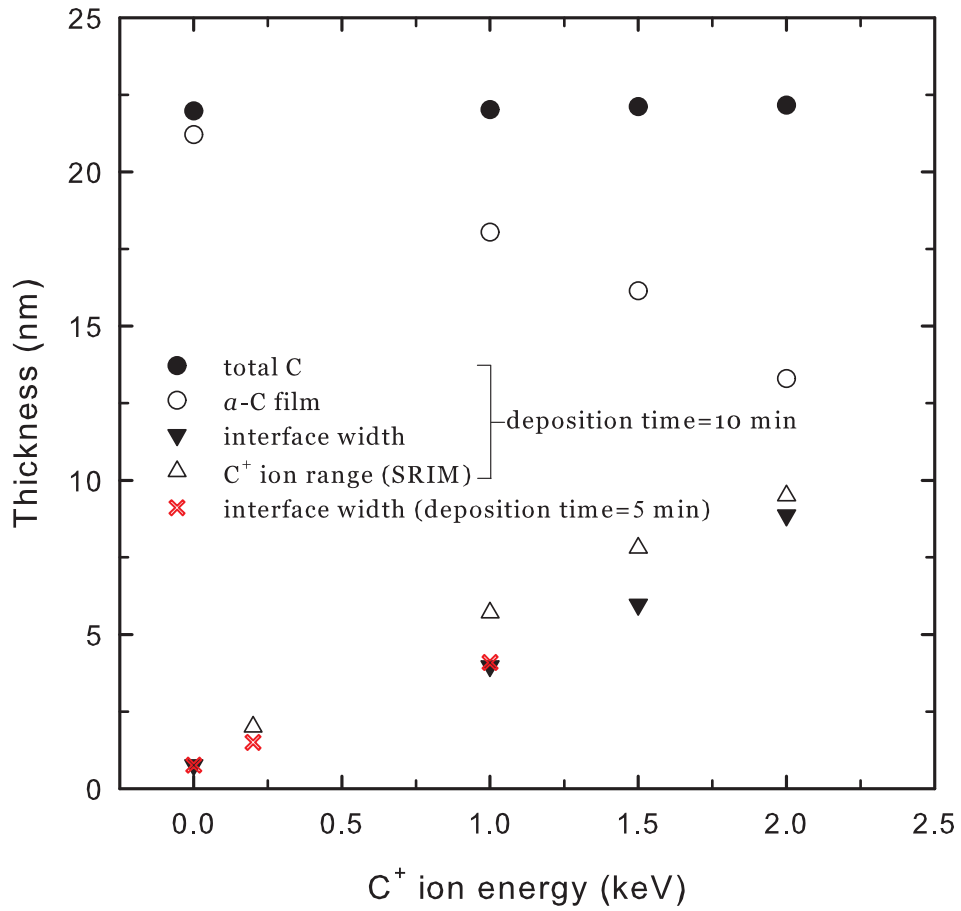


Fig. 5. The thickness of the *a*-C/Si interface and *a*-C film are plotted as a function of C<sup>+</sup>-ion energy. The corresponding C<sup>+</sup>-ion ranges calculated by SRIM are also included.

1  
2  
3  
4  
5  
6  
7  
8  
9  
10  
11  
12  
13  
14  
15  
16  
17  
18  
19  
20  
21  
22  
23  
24  
25  
26  
27  
28  
29  
30  
31  
32  
33  
34  
35  
36  
37  
38  
39  
40  
41  
42  
43  
44  
45  
46  
47  
48  
49  
50  
51  
52  
53  
54  
55  
56  
57  
58  
59  
60  
61  
62  
63  
64  
65

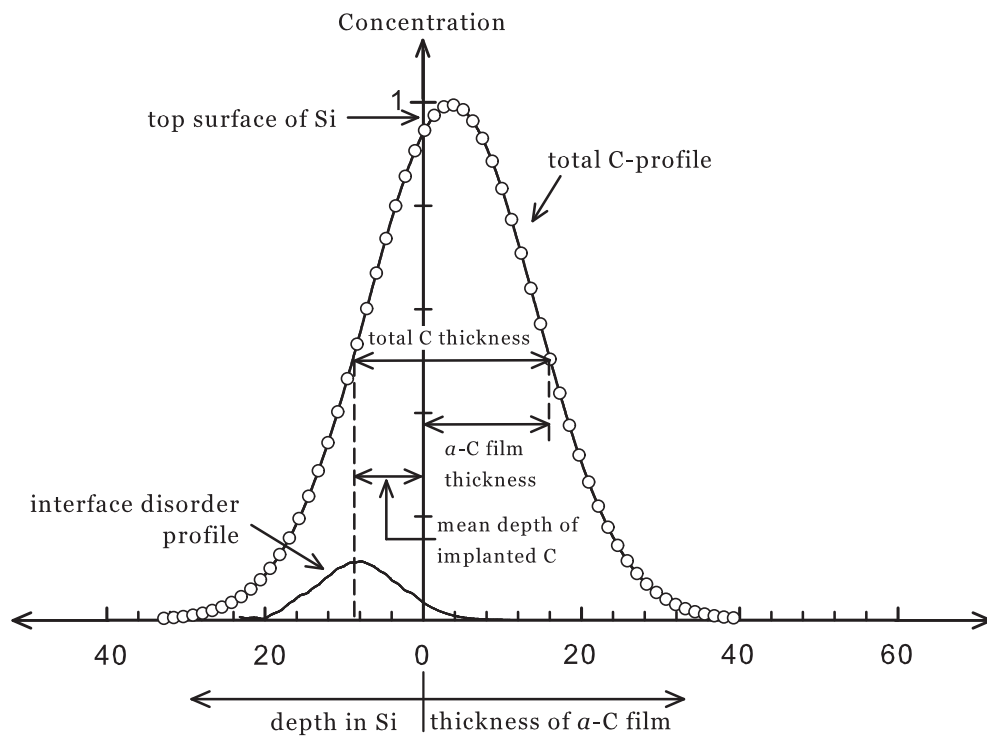


Fig. 6. Overview of *a*-C/Si interface structure containing the implanted carbon ions and displaced Si atoms together with the deposited *a*-C film.